

Article

# Concentration and Recovery of Valuable Heavy Minerals from Dredged Fine Aggregate Waste

Fausto Moscoso-Pinto <sup>1,2</sup> and Hyung-Seok Kim <sup>1,2,\*</sup>

<sup>1</sup> Mineral Resources Division, Resources Recovery Research Center, Korea Institute of Geoscience and Mineral Resources, Daejeon 34132, Korea; fausto@kigam.re.kr

<sup>2</sup> Department of Resources Recycling, University of Science and Technology (UST), Daejeon 34113, Korea

\* Correspondence: hskim@kigam.re.kr; Tel.: +82-42-868-3575

**Abstract:** Inside the finest fractions of aggregates, usually wasted by ready mix concrete companies, valuable heavy minerals content is substantial. The concentration and recovery of valuable heavy minerals contained in dredged fine aggregates waste, located in Pyeongtaek South Korea, were investigated to develop a process that can recover and concentrate most of each heavy mineral. The raw material contains ilmenite, magnetite, monazite, and zircon. A gravity separation, recirculating the middlings recovered ilmenite, magnetite, monazite, and zircon with 44.05%, 36.90%, 53.76%, and 69.7% respectively. Nevertheless, a magnetic separation followed by gravity separation of the non-magnetic fraction further improved the recovery of ilmenite, magnetite, monazite, and zircon to 86.96%, 85.09%, 91.06%, and 90.82% respectively. This concentrate was separated at different magnetic intensities. Magnetite was concentrated at 0.05 T, resulting in a recovery of 23.4% and grade of 95.1 wt%. Ilmenite was at 0.4 T, with a recovery of 55.2% and grade of 84.2 wt%. Monazite was at 0.9 T, with a recovery of 59.3% and rare earth oxide content of 45.2%, the non-magnetic fraction has a high zircon content, the recovery was 70.6% and grade of 91.8 wt%.

**Keywords:** valuable heavy minerals; VHM; fine aggregate waste; dredged fine aggregates; mineral processing; gravity separation; magnetic separation; zircon; monazite; ilmenite



**Citation:** Moscoso-Pinto, F.; Kim, H.-S. Concentration and Recovery of Valuable Heavy Minerals from Dredged Fine Aggregate Waste. *Minerals* **2021**, *11*, 49. <https://doi.org/10.3390/min11010049>

Received: 30 November 2020

Accepted: 30 December 2020

Published: 5 January 2021

**Publisher's Note:** MDPI stays neutral with regard to jurisdictional claims in published maps and institutional affiliations.



**Copyright:** © 2021 by the authors. Licensee MDPI, Basel, Switzerland. This article is an open access article distributed under the terms and conditions of the Creative Commons Attribution (CC BY) license (<https://creativecommons.org/licenses/by/4.0/>).

## 1. Introduction

Although the recycling of metals has become a global trend, this process does not cover the demand because they still have low recycling rates. Moreover, some metals such as titanium, rare earths elements (Ce, Nd, Dy, etc.), and zircon do not have effective substitutes. Hence, the exploration and exploitation of new mine resources for extracting these minerals are essential [1]. Besides, some new technology (electronic devices, electric vehicles, wind turbines, light alloys) needs some very specific metals without which this technology would have not developed as much as it has been. That is why, some minerals as monazite, xenotime, rutile, ilmenite, etc., are considered valuable heavy minerals. For example, in 2018 the U.S. imported 18,500 t of total rare earth elements (TREE), represented \$165 million [2], but China produced 70.59% of TREE in this year [3]. That makes TREE are considered critical metals for the European Union and U.S. Government [4,5]. TREE are essential metals in the production of cleaning energy. As this industry is continuously growing, the demand for REE minerals is increasing especially in the countries where high-technology is produced [5].

South Korea is being known as a world leader for the production of high-technology manufactured equipment and transportation (cars, ships, smartphones, etc.). However, the over-dependency on the imports of metals required to assemble these products, and the unreliable international market are severely affecting the country's growth. Besides, the construction industry has contributed considerably to the accelerated development of the Korean economy. It represents 5.9% of the Gross domestic product (GDP), around 22 billion Korean Won (KRW), or \$18 billion US Dollars (USD) [6]. It was reported that South Korea

is producing and exploiting aggregates to develop its building industry [7]. Route One Communications Ltd. pointed out that South Korea required 250 million cube meters of aggregates in 2016 for its infrastructure development [7]. Aggregates can be divided into two categories i.e., coarse and fine. The American Standard Test Method, in its normative C 33–03 for concrete aggregates, allows a relatively wide range in the granulometry of each one. Nonetheless, this normative restricts the fine aggregate, a determined fraction cannot pass 45% of any sieve, and be retained in the next consecutive sieve [8]. Moreover, the normative provides limits to the retained fraction for concrete aggregates [8,9].

For accomplishing the normative, ready mix concrete (RMC), companies need to sieve fine particle aggregates, producing big amounts of waste. By contrast, the finest particles of sands and placer deposits have a considerable content of valuable heavy minerals (VHM), such as hematite, ilmenite, magnetite, monazite, rutile, zircon, etc. [10–17]. Additionally, even sands and placer deposits could have a relatively low concentration of heavy minerals, comparing with other mineral sources, the large volume these represent in the construction industry makes these deposits potentially attractive for being processed [10]. Some studies have recovered and separated heavy minerals from beach sands [11–13], dredged sediments [14], and placer deposits [15,16]. Frihy et al. [12] demonstrated that when dredged sediments have a concentration greater than 2 wt% of heavy minerals, the deposit is economically profitable.

Most of the physical beneficiation involving sands or aggregates begins with a gravity separation in order to isolate heavy minerals from gangue, which are mainly composed of quartz [17–19]. Normally, these minerals do not need comminution, reducing the processing costs, and saving energy [20]. After gravity separation, heavy minerals can be separated by magnetic separation, electrostatic separation, or flotation, depending on the characteristics of each mineral to be separated [13,16–21]. About magnetic separation, the mining industry is currently the largest sector using this process for ore treatment, material sorting, and purification of minerals [22]. Therefore, it is essential to decide on the mineral processing that can recover the most VHM, with a fast and efficient processing rate.

This research aimed to recover and concentrate the valuable heavy minerals from a dredged fine aggregate waste, which was collected next to a river in Pyeongtaek, South Korea. Among their valuable minerals, we can find hematite, magnetite, ilmenite, monazite, and zircon. For achieving the recovery and concentration of VHM, this study compared two different mineral processes: gravity and magnetic separation. The final concentrate was separated at different magnetic field intensities to improve the recovery and final grade of each VHM.

## 2. Materials and Methods

### 2.1. Background (Study Area)

The sands used in this work were dredged at 36°56'25" north latitude and 126°59'23" east longitude, next to a river in Pyeongtaek, which is located in the southwestern part of Gyeonggi Province, South Korea. These sands were dredged for producing coarse and fine aggregates. Figure 1 describes the procedure of separation. The sands are dredged and sieved by a trommel at 7 mm, and the fraction retained is used as coarse aggregates. Then a wet cyclone separates the slime (overflow of the cyclone) from the aggregate (underflow of the cyclone) which is sieved again at 1 mm. The retained fraction is considered as fine aggregate. Coarse and fine aggregates are transported to the RMC.

The fraction with particle lower than 1 mm is considered as a fine aggregate waste since it cannot be used as concrete aggregates. Nonetheless, as described earlier, it has a considerable amount of VHM, hence, it was used as the raw material in this work (hereinafter, referred to as "fine aggregate waste"). Around 100 t of the fine aggregate waste ( $d_{80} = 300 \mu\text{m}$ ) were collected for the mineral processing of this work. The sample was dried, mixed, and divided to sample it for the chemical and mineral analysis.

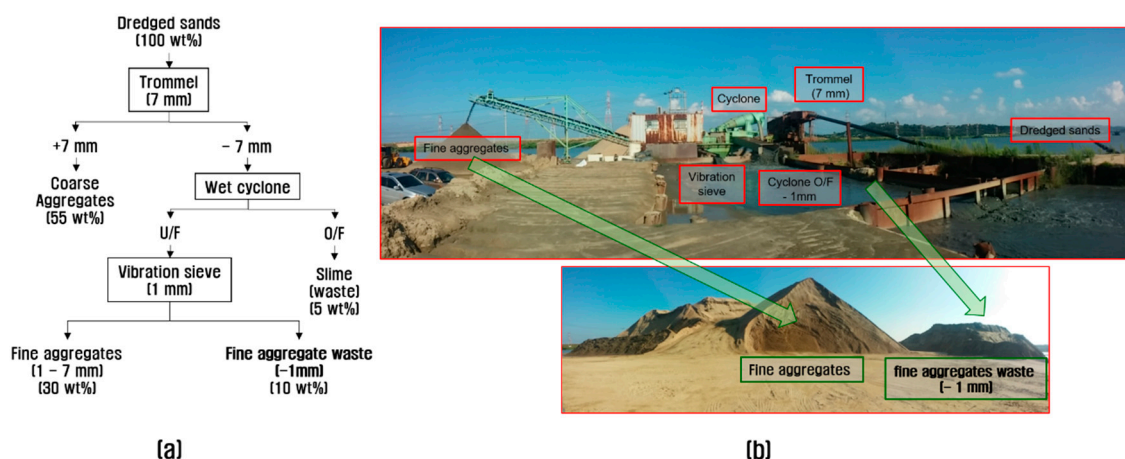


**Figure 1.** Production of coarse and fine aggregates by dredging sands: (a) simplified flow sheet, (b) photographs of the actual process.

The chemical composition and particle size distribution of the fine aggregate waste are shown in Table 1. The principal mineral contained in the raw material is quartz (SiO<sub>2</sub>); however, the fraction smaller than 300 μm has a considerable amount of ZrO<sub>2</sub> (0.11 wt%), TiO<sub>2</sub> (0.56 wt%), and Fe<sub>2</sub>O<sub>3</sub> (2.94 wt%); this could represent valuable minerals (hematite, magnetite, ilmenite, zircon among others). From a particle size of 150 μm, the content of ZrO<sub>2</sub>, TiO<sub>2</sub>, and P<sub>2</sub>O<sub>5</sub> (could represent monazite) increases. Additionally, Table 1 shows the total heavy mineral content of each sieved fraction. When the particle size of the fine aggregate waste decreases, the total heavy mineral content increases. Moreover, the fraction bigger than 600 μm only consisted of 0.06 wt% of heavy minerals, while the fraction between 75 μm and 43 μm has 6.60 wt%. Indeed, the fine aggregate waste has 3.25 wt% of heavy mineral.

**Table 1.** Particle size distribution and chemical composition of each particle size fraction of the dredged fine aggregate waste from Pyeongtaek, used as raw material.

Particle Size Distribution (μm)	Mass Fraction (wt%)	Total Heavy Mineral Content * (wt%)	Chemical Composition (wt%)												LOI **
			SiO <sub>2</sub>	Al <sub>2</sub> O <sub>3</sub>	Fe <sub>2</sub> O <sub>3</sub>	CaO	MgO	K <sub>2</sub> O	Na <sub>2</sub> O	TiO <sub>2</sub>	MnO	P <sub>2</sub> O <sub>5</sub>	ZrO <sub>2</sub>		
−1000 + 600	8.92	0.06	88.67	4.99	0.44	0.27	0.13	3.41	0.86	0.07	0.01	0.02	0.00	0.77	
−600 + 300	10.62	0.24	85.74	6.68	1.14	0.45	0.28	3.19	1.15	0.17	0.02	0.04	0.01	0.95	
−300 + 150	12.06	1.26	77.17	11.19	2.54	0.91	0.63	3.42	1.79	0.36	0.04	0.07	0.04	1.60	
−150 + 75	34.19	4.48	76.13	11.57	2.74	1.04	0.76	3.33	2.05	0.40	0.04	0.08	0.08	1.59	
−75 + 43	19.93	6.60	75.41	11.57	2.96	1.30	0.90	2.87	2.21	0.65	0.05	0.11	0.15	1.61	
−43	14.29	1.51	73.13	12.05	3.75	1.42	1.03	2.59	2.18	0.99	0.07	0.15	0.22	2.36	
TOTAL (raw)	100.0	3.25	77.82	10.49	2.53	1.00	0.70	3.14	1.87	0.48	0.04	0.09	0.09	1.56	

\* The total heavy mineral content was determined by heavy liquid separation using 1,1,2,2-tetrabromoethane (C<sub>2</sub>H<sub>2</sub>Br<sub>4</sub>). \*\* Loss on ignition.

### 2.2. Characterization of the Fine Aggregate Waste

The fine aggregate waste was analyzed by an X-ray diffractometer (XRD; Bruker D8 Advance A25, Bruker-AXS, Mannheim, Germany). The diffractogram was obtained for 2θ values from 5 to 65°. A divergence slit of 0.3°, a Soller slit of 2.5°, and a sample rotation speed of 20 RPM. Additionally, the particle size was determined by a sieving test in wet medium and the chemical composition of every fraction was analyzed by an X-ray fluorescence spectrometer (XRF; XRF-1800, Shimadzu, Kyoto, Japan).

Figure 2 shows the X-ray powder diffraction patterns of the fine aggregate waste. It shows that the main component was quartz (SiO<sub>2</sub>; JCPDS 46-1045), corroborating the results with Table 1. It was obvious since the dredged aggregates are sands. Nonetheless, some other gangue was observed such as hornblende (Ca<sub>2</sub>Mg<sub>4</sub>Al<sub>0.75</sub>Fe<sub>0.25</sub>(Si<sub>7</sub>AlO<sub>22</sub>)(OH)<sub>2</sub>; JCPDS 01-071-1060), albite (NaAlSi<sub>3</sub>O<sub>8</sub>; JCPDS 09-0466), and muscovite (Al<sub>3</sub>KSi<sub>3</sub>O<sub>10</sub>(OH)<sub>2</sub>;

JCPDS 01-080-0743). As the content of possible VHM was not visible, the diffractogram was magnified as shown in Figure 2b to highlight small peaks. Figure 2b shows hastingsite ( $\text{NaCa}_2\text{Fe}_5(\text{Si}_6\text{Al}_2\text{O}_{22})(\text{OH})_2$ ; JCPDS 01-085-1423), zircon ( $\text{ZrSiO}_4$ ; JCPDS 06-0266), and ilmenite ( $\text{FeTiO}_3$ ; JCPDS 29-0733) with low intensity peaks; however, this consideration cannot be ascertained since it was only the main peak of each mineral and it was inconsiderable.

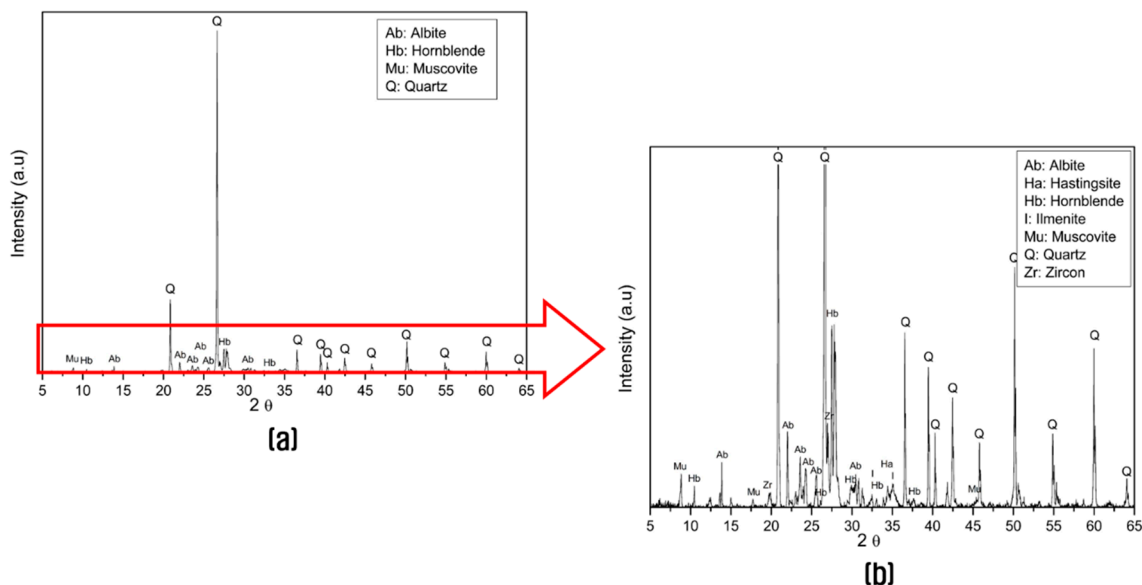


**Figure 2.** X-ray powder diffraction patterns of (a) the fine aggregate waste and (b) five times magnification of the patterns.

A heavy liquid separation test was prepared, using 1,1,2,2-tetrabromoethane ( $\text{C}_2\text{H}_2\text{Br}_4$ ), which has a density of  $2.97 \text{ g/cm}^3$  with the purpose of separating the valuable heavy minerals (densities are between  $3.5$  and  $5.7 \text{ g/cm}^3$ ) from the gangue, principally formed by quartz (density of  $2.66 \text{ g/cm}^3$ ). Moreover,  $250 \text{ g}$  of each sieved fraction was transferred in a separation funnel with the heavy liquid, stirred for  $5 \text{ min}$  and was allowed to stand for  $1 \text{ h}$ . After this time, heavy (sink) and light (float) fractions were separated, rinsed with acetone, dried, and weighed. Each heavy fraction was analyzed by XRD. Additionally, the content of total rare earth element (TREE) and degree of liberation of the VHM contained in the heavy fraction of the fine aggregate waste was analyzed by inductively coupled plasma mass spectroscopy (ICP-MS; Elan DRC-II, Perkin Elmer, Waltham, MA, USA) and a mineral liberation analyzer (MLA; MLA650F, Thermo-Fisher Scientific, Hillsboro, OR USA) operated at  $25 \text{ kV}$  and a beam current of  $5 \text{ nA}$ , respectively.

### 2.3. Concentration of the Valuable Heavy Minerals by Gravity Separation and Magnetic Separation

Most of the mineral processing involving sand begins with gravity separation [10,14,16,23] owing to the density difference with the gangue (mostly quartz). Moreover, any physical beneficiation, which includes sands and placer deposits for concentrating heavy minerals, needs to have the capability to treat big amounts of the raw material to be commercially viable. Typically tonnages are from  $3.3$  million tons to  $8.5$  million tons annually [24,25]. Thereby, spiral concentrators are used as a first step of the concentration [16,23].

Considering that the concentrate was not sufficient for the subsequent mineral processing, it was necessary to process a considerable amount of the fine aggregate waste, at a pilot scale for obtaining representative data. Therefore, a pilot-scale Humphrey spiral concentrator located in the Korea Mining Development Company (Jecheon, Korea) was preferred. The spiral concentrator is  $4 \text{ m}$  high and it has six windings (MD Mineral Technologies, Queensland Australia). Figure 3 shows some photos of the pilot spiral concentrator. Additionally, Figure 3 illustrates a layout of the gravity separation route used in this work. The fine aggregate waste as received was fed at  $2000 \text{ kg/h}$  (dry base),  $15 \text{ wt\%}$  of solids. It

was found that at these conditions, the heavy minerals, were reasonably well separated based on a series of preliminary experiments at a laboratory scale with a five windings spiral concentrator (MD Mineral Technologies, Queensland, Australia). The concentrate and tailings were dried and weighed before chemical characterization such as XRF and ICP-MS. Additionally, a series of experiments considered the recirculation of middlings to enhance the recoverability of the VHM.

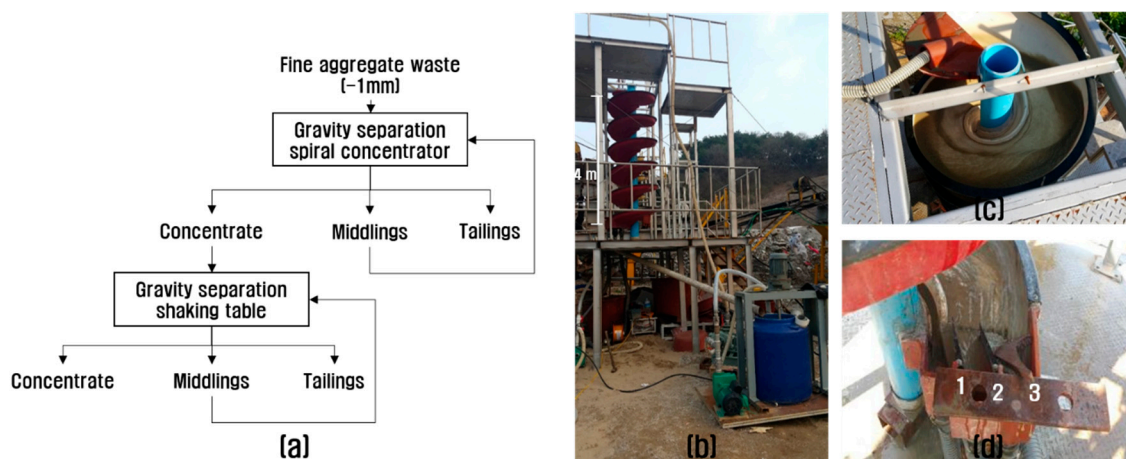


**Figure 3.** (a) Layout of the gravity separation path, and photographs of the pilot scale Humphrey spiral used in this work: (b) general view of the spiral concentrator; (c) plan view of the spiral once it was placed sample; (d) collection of the concentrate (1), middlings (2), and tailings (3).

Due to the presence of impurities, such as quartz and hornblende in the concentrate, proper cleaning was required which was done by a pilot-scale shaking table (4.7 m × 1.67 m) located in the Korea Mining Development Company (Jecheon, Korea). The spiral concentrate was fed in the shaking table at 1100 kg/h (dry base), 5 wt% of solids, 300 strokes, and an inclination angle of 0.4°, which are the same conditions as the preliminary laboratory experiments using a shaking table No 13 Wilfley (Wilfley®, Humphreys, Jacksonville, FL, USA). Concentrate and tailings were dried and weighed, followed by chemical analyzed using XRF. The content of TREE was determined by ICP-MS. Further, a series of experiments were conducted regarding the recirculation of middlings to enhance the recoverability of the VHM as is shown in Figure 3a. Moreover, Figure 4 shows some photographs of the pilot shaking table used in this work.

Some studies have used gravity separation as the first step for the concentration of heavy minerals in placer deposits or dredged sands, while others have begun with a magnetic separation as a first processing stage [13]. The reason is the magnetic susceptibility that most of the heavy minerals have, excluding zircon, comparing with the diamagnetic character of quartz [26,27]. Therefore, the VHM contained in the fine aggregate waste were concentrated by magnetic separation using a vortex type super magnetic coolant separator (VMCS, Dae Bo Magnetic Co., LTD., Hwasung-Si, Korea) located in the Korea Mining Development Company (Jecheon, Korea). The magnetic separator was fed at 2000 kg/h (dry base), 10 wt% of solids. The roll speed was 50 RPM and the magnetic field intensity was 0.9 T. These conditions were selected following a series of preliminary tests using a laboratory-scale magnetic roll (L/P10.30), designed by a patent at 1.2 T [28]. Magnetic and non-magnetic fractions were weighed and chemically analyzed by XRF and content of TREE was determined by ICP-MS. As a final point, the non-magnetic fraction, which has a considerable percentage of zircon, was subjected to gravity separation, thereby increasing the recovery of zircon using the pilot spiral concentrator with the same conditions as described above (2000 kg/h dry base and 15 wt% solids). With all the collected data, a preliminary flow sheet was designed for the concentration of VHM contained in the dredged aggregate waste, which is shown in Figure 5. The final concentrate post magnetic separation and gravity separation of the non-magnetic fraction was cleaned again by

gravity separation using a shaking table to remove some residual gangue. This final concentrate fraction will be referred to henceforth as the final concentrate.

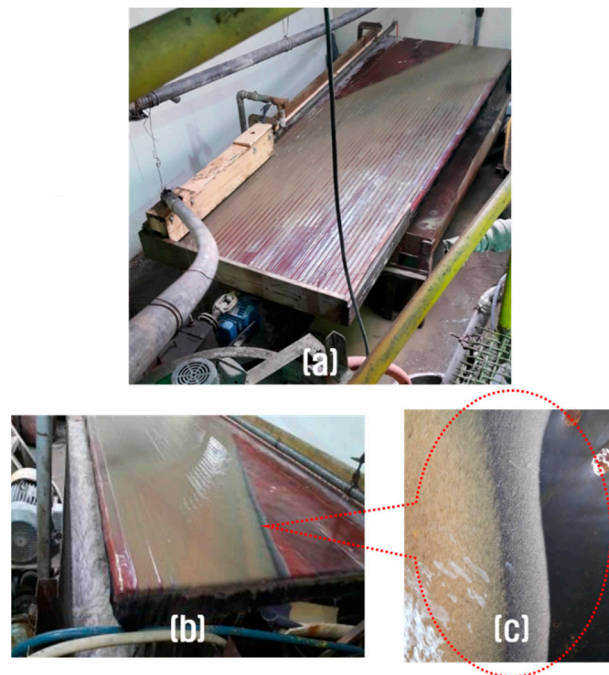


**Figure 4.** Photographs of the pilot scale shaking table used in this work: (a) general view of the shaking table, (b) collecting of the concentrate and tailings, (c) concentrate and tailings of the scrubbed fine aggregate waste.

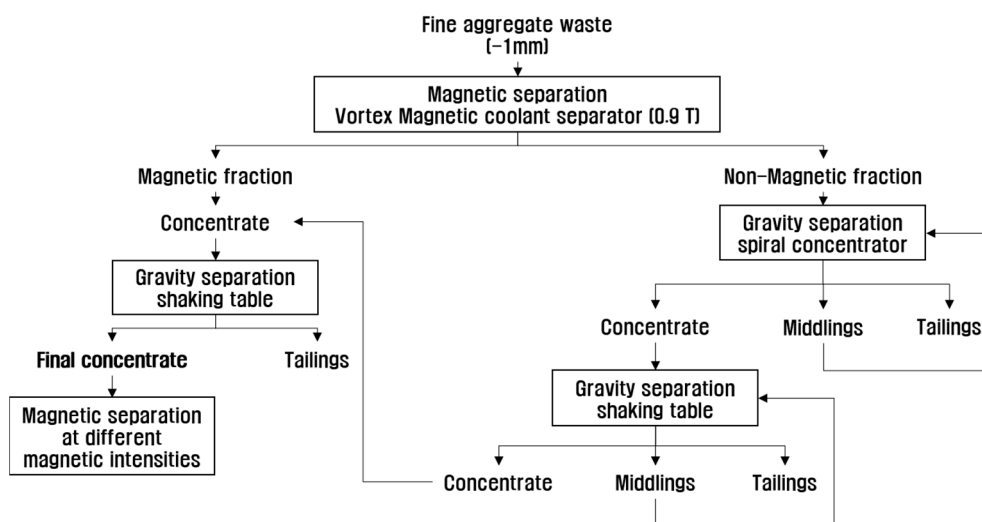


**Figure 5.** Preliminary flow sheet for the concentration of valuable heavy minerals (VHM) from fine aggregate waste.

#### 2.4. Separation of Each Valuable Heavy Mineral by Magnetic Separation at Different Magnetic Intensities

The final concentrate was separated at different magnetic field strength to determine the optimum conditions for the extraction of each VHM contained in it. For achieving that, a laboratory-scale cross-belt magnetic separation (HCB 7-11-2, Eriez, PA, USA) was used. It can modulate the applied magnetic field intensity by changing the voltage of the electromagnet or the height between it and the cross-belt conveyor. However, the magnet’s

height was fixed at 1 cm since the voltage was deemed to be a more convenient way to control the magnetic intensity.

2 kg of the final concentrate was fed at 100 g/min. The magnetic field intensity was increased from 0.05 T to 1.2 T and measured with a teslameter (TM-197, Tenmars, Taipei City, Taiwan). After recovering and removing the magnetic products, the non-magnetic fraction was reprocessed at an increased magnetic intensity. The chemical composition and TREE content were determined by XRF, and ICP-MS, respectively. Then, 10 kg of the final concentrate was separated at the predetermined magnetic intensities to recover each VHM. Firstly, the magnetite and hematite were separated at a very low magnetic flux density (0.05 T). Ilmenite was separated at 0.4 T. After that, monazite was separated at 0.9 T. Finally, the 0.9 T non-magnetic fraction has a high zircon concentration. As a final point, since the ilmenite concentrate and the monazite concentrate picked up some impurities such as hornblende and muscovite, each valuable mineral was purified by gravity concentration. Zircon was also separated from quartz using the same separation process. The concentrate and tailings of each fraction were analyzed by XRF and XRD. Considering all the collected data, a process flow diagram was suggested for recovering and concentrating most of each VHM from the fine aggregate waste.

### 3. Results and Discussion

#### 3.1. Characterization of the Fine Aggregate Waste

The fine aggregate waste heavy fraction and each sieved heavy fractions were separated through a heavy liquid separation, and they were analyzed through XRD as depicted in Figure 6. According to the X-ray powder diffraction patterns of Figure 6, the heavy fraction of the raw material shows ilmenite, magnetite ( $\text{Fe}_3\text{O}_4$ ; JCPDS 19-0629), monazite ((Ce, La, Nd) $\text{PO}_4$ ; JCPDS 46-1295), quartz and zircon. Each mineral was indistinctively present in each heavy fraction. Nonetheless, Figure 6 shows that the zircon was more concentrated in heavy fractions at small particle sizes, corroborating the results with Table 1. Contrary to what may be expected, Figure 6 showed that the quartz content was considerable even when the objective of the heavy liquid separation test was to try to eliminate it. The probable reason can be the degree of liberation, which may not be particularly good; hence, a mineral liberation analysis (MLA) was required.

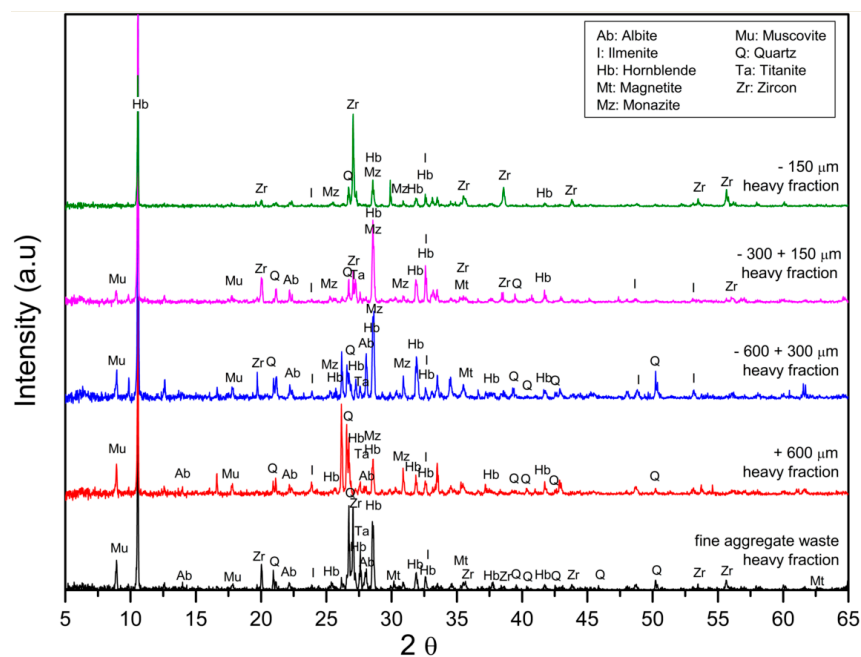


**Figure 6.** X-ray powder diffraction patterns of the heavy fraction, separated by 1,1,2,2-tetrabromoethane ( $\text{C}_2\text{H}_2\text{Br}_4$ ), of the fine aggregate waste and its respectively sieved fractions.

Likewise, the heavy fraction has albite, hornblende (density 3–3.47 g/cm<sup>3</sup>), and titanite (CaTiSiO<sub>5</sub>; JCPDS 01-071-1157; density 3.48–3.6 g/cm<sup>3</sup>) as impurities. Recent studies have verified hornblende in heavy sands and placer deposits [10,14,16,29]. Lee, Cho, and Yi [29] found concentrations of hornblende attached to ilmenite and a little percentage of zircon. Although the chemical composition of Table 1 did not show the occurrence of monazite, the XRD patterns confirm the presence of this heavy mineral in the raw material. The percentage of P<sub>2</sub>O<sub>5</sub> in the chemical composition could indicate the presence of this valuable mineral but in small quantities.

The MLA analysis of the heavy fraction of the fine aggregate waste is shown in Figure 7a. This analysis confirmed the mineral composition of the heavy minerals in the fine aggregate waste. According to Figure 7a, the principal VHM are magnetite (red), ilmenite (green), monazite (fuchsia), and zircon (cyan). Figure 7a shows quartz (peach), muscovite (grey), hornblende (sky blue), oxides (yellow), and other phosphates (purple). Additionally, Figure 7b shows the liberation percentage expressed in cumulative weight of the four main valuable heavy minerals. Particles can be classified into three groups according to their liberation ratio, i.e., free particles (liberation ratio higher than 95%), liberated particles (liberation ratio between 80 to 95), and locked particles (liberation ratio lower than 80%) [18,30,31]. Thus, Figure 7b expresses liberated and non-liberated (locked) particles. Each VHM has an acceptable liberation rate since they were aggregates from placer deposits; it means they were weathered and concentrated during long periods by water bodies. The raw material was extracted next to the river as shown in Figure 1. Conversely, the ratio of ilmenite (82.0%) was lower than expected for these kinds of dredged sands and placer deposits [16]. As Figure 7a shows, ilmenite was attached to hornblende and muscovite. This can be the reason why muscovite was present in the heavy fraction, although its density is lower than the heavy liquid (2.83 g/cm<sup>3</sup>). Alternatively, magnetite (95.1%) and zircon (98.0%) are well liberated. Finally, Table 2 summarizes the mineral composition obtained by modal mineralogy through MLA. If Table 2 was compared with the XRD of the heavy fraction of the fine aggregate waste, shown in Figure 6, the results matched. If Table 2 was compared with Figure 7b, the unusual content of quartz does not have a relationship with the liberation degree of VHM since the VHM particles were liberated. Thus, quartz could be attached to hornblende. Certainly, Kato found quartz spots in hornblende [32].

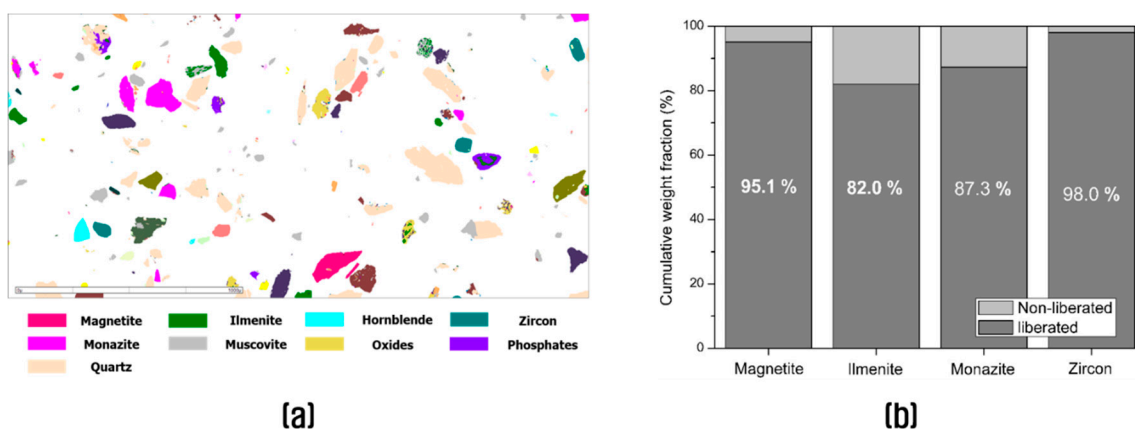


**Figure 7.** Mineral liberation analysis (a) heavy fraction of the fine aggregate waste (b) degree of liberation of the main VHM in the sample.

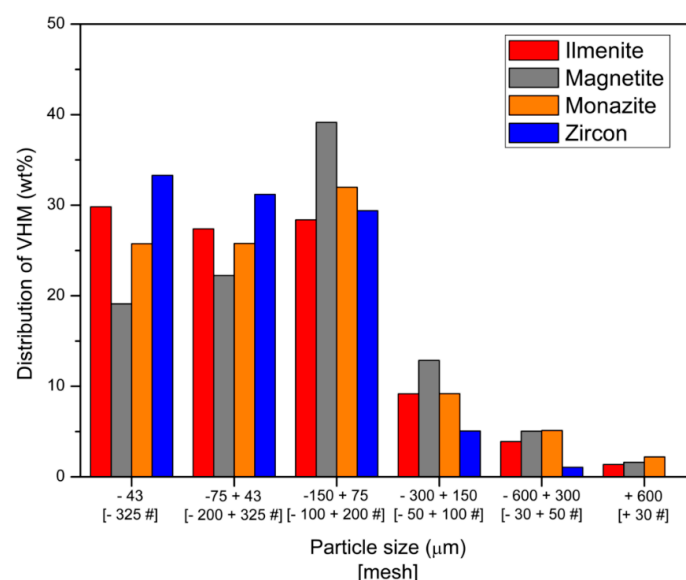


**Table 2.** Mineral composition of the heavy fraction of the fine aggregate waste, analyzed by modal mineralogy defined by mineral liberation analysis (MLA).

Mineral	Fraction (wt%)	Mineral	Fraction (wt%)
Ilmenite	30.2	Magnetite	24.6
Monazite	1.3	Hornblende	21.7
Zircon	5.3	Oxide	5.1
Muscovite	0.2	Phosphates	1.4
Quartz	10.1	Others	0.2

The contents of magnetite, ilmenite, and zircon in the fine aggregate waste were calculated, assuming all the VHM were recovered by heavy liquid separation. Thus, the raw material has 0.98 wt% of ilmenite, 0.80 wt% of magnetite, 0.18 wt% of zircon. Moreover, the monazite content was determined by applying ICP-MS to the heavy fraction of the fine aggregate waste post calcination with  $\text{Na}_2\text{O}_2$  and was recorded 618.4 ppm. If the monazite content in the fine aggregate waste was determined by the mineral content in Table 2, it would be 422.5 ppm; however, the ICP-MS analysis determined a bigger monazite content. The difference could be in the phosphates content showed in Table 2. Nevertheless, it was decided to accept the value provided by ICP-MS since it was a direct form of analysis.

If the  $\text{ZrO}_2$  content of Table 1 is assumed to be the content of zircon ( $\text{ZrSiO}_4$ ) in the fine aggregate waste, the calculated value is comparable with the value from Table 2 (0.18 wt% by MLA and 0.15 wt% by XRF). For comparison, the ilmenite content can also be calculated from the  $\text{TiO}_2$  content in Table 1. Nonetheless, since hornblende has titanium, this titanium content in hornblende should be removed for determining a more accurate percentage of ilmenite, even so, the results were corresponding (0.98 wt% by MLA and 0.90 wt% by XRF). To conclude, Figure 8 shows the particle distribution of each VHM in the fine aggregate waste. As can be seen, the fraction bigger than 0.6 mm does not have as much of the heavy minerals as the other fractions. Indeed, the percentage of zircon was almost null. Besides, at smaller fractions, the valuable minerals content increases, as confirmed from the chemical composition of each particle size in Table 1.

**Figure 8.** Weight distribution of the principal VHM contained in the raw material. VHM content: ilmenite = 0.98 wt%, magnetite = 0.80 wt%, zircon = 0.18 wt%, monazite = 618.4 ppm.

### 3.2. Concentration of the Valuable Heavy Minerals by Gravity Separation and Magnetic Separation

Figure 9a shows the results for the Humphrey spiral concentrator when the splitter, pointed in Figure 3d, was moved to obtain more concentrate fraction. Additionally, the recirculating

of middlings was applied as it is shown in Figure 3a for increasing the recovery of VHM. The results are in Figure 9b. As expected, when more concentrate was recovered, the VHM content also increases. In addition, Figure 9b demonstrates the improvement of the recovery of VHM contained in fine aggregate waste. Comparing Figure 9a with Figure 9b, when the middlings was recirculated, the recovery of VHM increased at the same wt% retained. Consequently, a recirculation of middlings significantly increases the recovery of VHM.

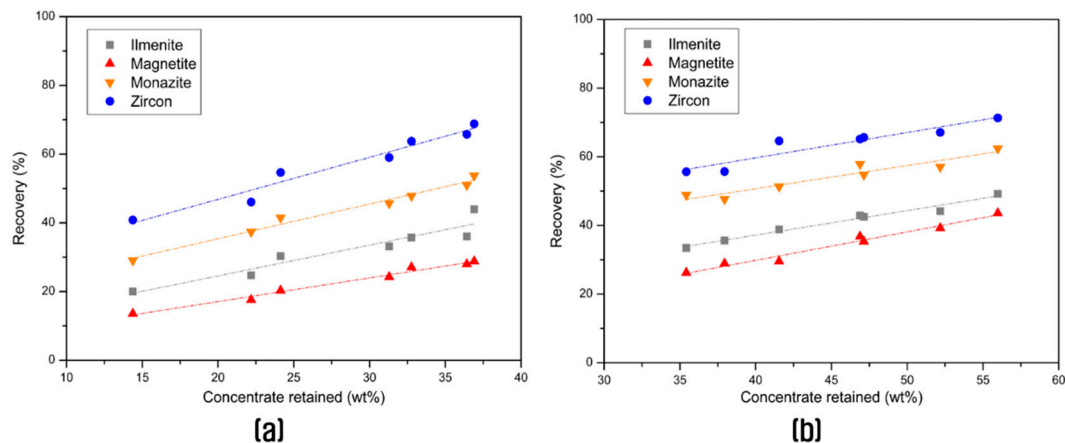


**Figure 9.** Recovery of VHM contained in the fine aggregate wastes by gravity separation using Humphrey spiral concentrator (a) concentrate retained (wt%) without recirculation, (b) concentrate retained (wt%) with recirculation of the middlings.

After the spiral concentrator, a cleaning of the concentrate was required for removing the gangue, principally quartz, hornblende, and muscovite. Therefore, the second stage of gravity separation was a shaking table. Some other works have done a gravity separation as first stage, followed by a shaking table of the concentrate [1,16]. Moreover, the recirculation of middlings was once again evaluated. The results are in Figure 10a when middlings was not recirculated, and Figure 10b, when the middlings was recirculated, as it is pointed in Figure 3a. As it was expected, Figure 10b shows a better recovery of heavy minerals when middlings was recirculated into the shaking table. Moreover, it reduces considerably the weight of the concentrate. Thus, recirculation of the middlings allows significant increases in the recovery of VHM.

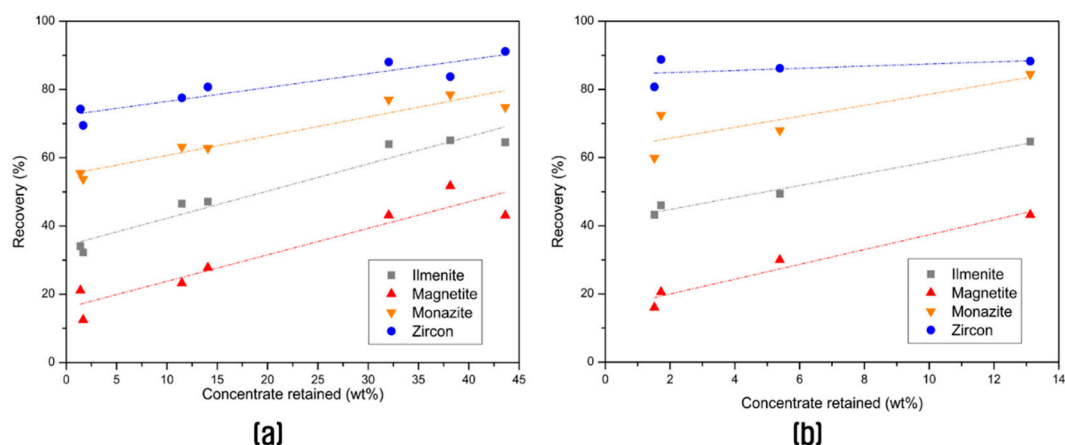


**Figure 10.** Recovery of VHM contained in the fine aggregate wastes by gravity separation using shaking table (a) concentrate retained (wt%) without recirculation (b) concentrate retained (wt%) with recirculation of middlings.

As the conditions of the preliminary laboratory tests and pilot-scale tests were different, specifically at the magnetic separation, the recovery of each heavy mineral was compared. The results are in Figure 11. As expected, gravity separation using the laboratory Humphrey spiral concentrator presented similar recovery rates than the pilot-scale recovery using a

similar concentrator at the same conditions established by laboratory tests. However, such as the magnetic roll in the preliminary laboratory tests has a stronger magnetic intensity (1.2 T comparing with 0.9 T of the pilot-scale magnetic roll), Figure 11a shows a better recovery of zircon (60.12%) comparing with 47.15% using the pilot-scale magnetic roll. Conversely, as the other VHM (magnetite, ilmenite, and monazite) are ferromagnetic or paramagnetic, a magnetic intensity of 0.9 T is sufficient for recovering them. The difference between these heavy minerals at laboratory and pilot-scale tests is negligible. Finally, when a magnetic separation and further gravity separation of the non-magnetic fraction was tested, the results coincided, emphasizing the scalability and importance of preliminary laboratory tests.

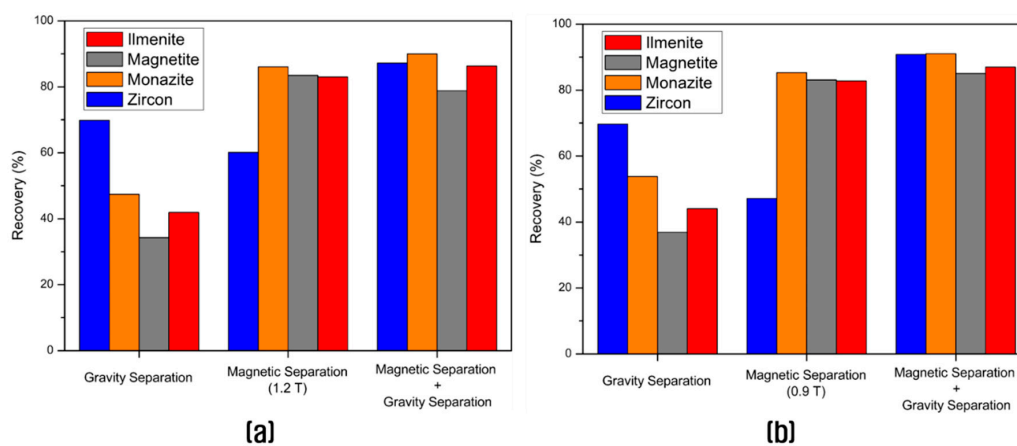


**Figure 11.** Recovery of each VHM in the fine aggregate wastes by gravity separation using the Humphrey spiral concentrator and magnetic separation using the magnetic roll (a) preliminary laboratory tests, (b) pilot-scale tests at the Korea Mining Development Company.

The grade and recovery rate of the fine aggregate waste using gravity separation were summarized in Table 3. The grade of each mineral was calculated from XRF considering that nearly all the  $TiO_2$  represents ilmenite, all the  $ZrO_2$  represents zircon, and that magnetite includes the  $Fe_2O_3$  content after subtracting the iron content from ilmenite. Even Humphrey spiral concentrator reduced the feed to 35.4 wt%, the recovery rate was very low. When the fine aggregate waste was not recirculated, the recovery rate of zircon was 57.03%, monazite 48.79%, ilmenite 35.76%, and magnetite 26.55%. Nevertheless, recirculation of the middlings increased the concentrate to 36.9% but the recovery rate increased in magnetite to 36.90%; ilmenite to 44.05%; monazite to 53.76%, and zircon to 69.7%. The principal problem that gravity separation holds was the recovery of magnetite and ilmenite.

**Table 3.** Grade and recovery of each heavy mineral in fine aggregate waste by gravity separation and magnetic separation.

	Mass Concentrate (wt%)	Grade (wt%)				Recovery (%)			
		Ilmenite	Magnetite	Monazite *	Zircon	Ilmenite	Magnetite	Monazite	Zircon
Fine Aggregate Waste		0.98	0.80	618.4	0.18				
Humphrey spiral	35.4	0.99	0.60	852.3	0.29	35.76	26.55	48.79	57.03
Spiral + Shaking table	11.5	1.85	0.80	2224.8	0.77	21.71	11.50	41.37	49.19
Spiral (recirculation of middlings)	36.9	1.17	0.80	901.0	0.34	44.05	36.90	53.76	69.70
Spiral + Shaking table (recirculation of middlings)	13.1	2.13	0.97	2142.9	0.83	28.47	15.88	45.39	60.41
Magnetic Separation	20.7	3.92	3.21	2548.6	0.41	82.80	83.06	85.31	47.15
Magnetic Separation + Gravity Separation (see Figure 5)	26.8	3.18	2.54	2101.2	0.61	86.96	85.09	91.06	90.82

\* Expressed in ppm.

Since magnetite is naturally ferromagnetic and considering the magnetic susceptibilities of monazite and ilmenite [27], a magnetic separation of the fine aggregate waste using a vortex type super magnetic coolant separator at 0.9 T was prepared. The results are shown in Table 3. Magnetic separation can concentrate most of the heavy minerals in the fine aggregate waste; however, the recovery of zircon was lower (47.15%) compared with the value obtained by gravity separation (60.41%). Notwithstanding, this value was unexpected considering the diamagnetic character of this mineral. The association of zircon with hornblende, a paramagnetic mineral, can promote magnetization and its further concentration [27]. Jordens et al. [31] found that zircon, allanite, and bastnasite either experienced enough magnetic force for being elevated or were recovered as mixed minerals, not totally liberated, and thus can be concentrated in the magnetic fraction. Moreover, since zircon was the most expensive mineral among the minerals contained in the raw material, its recovery can be essential [33]. Consequently, a gravity separation with recirculation of the middlings was required after the magnetic separation as pointed in Figure 5. When a magnetic separation and gravity separation of the non-magnetic fraction was made, the recovery rate of magnetite was 85.09%, ilmenite 86.96%, monazite 91.06%, and zircon 90.82%. This concentrate was again cleaned by gravity separation for reducing the quartz and hornblende content.

The final concentrate was analyzed using XRD and the results are shown in Figure 12. Even though the VHM tended to be separated from the gangue, some impurities such as hornblende, hastingsite, titanite, and quartz were confirmed in the concentrate. In addition, if the XRD patterns of Figure 12 are compared with the heavy fraction of the raw material shown in Figure 6, the final concentrate does not have as much hornblende and hastingsite as the raw material has, indicating the potential efficiency of the selected physical beneficiation.

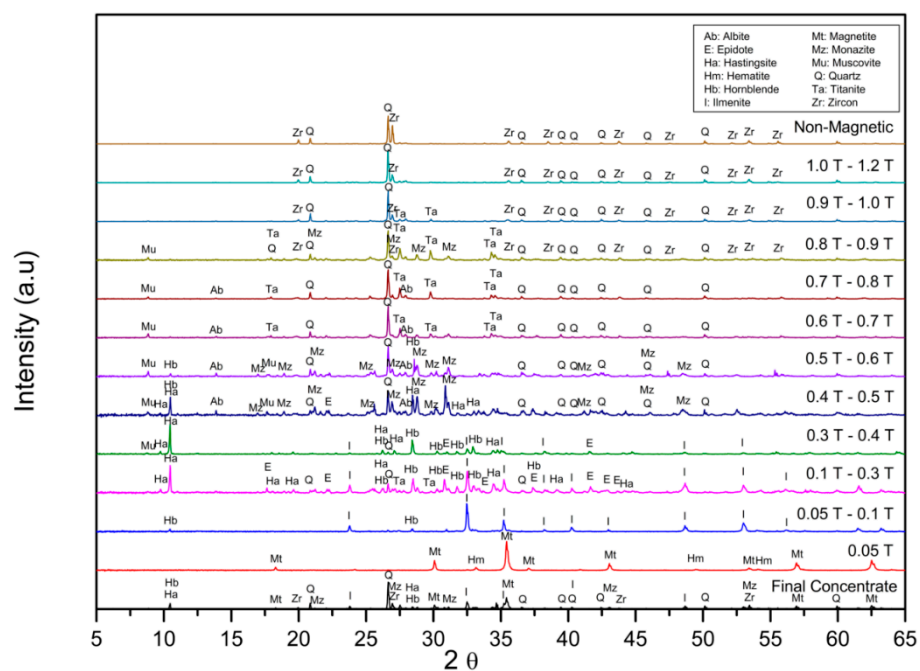


Figure 12. X-ray powder diffraction patterns of the magnetic separation at different magnetic intensities of the final concentrate.

### 3.3. Separation of Each Valuable Heavy Mineral by Magnetic Separation at Different Magnetic Intensities

Each heavy mineral has different magnetic characteristic and magnetic susceptibilities [27]. Therefore, the final concentrate was separated at different magnetic intensities. The XRD patterns of each fraction are shown in Figure 12. Figure 12 shows that magnetite was well concentrated at 0.05 T. Magnetite is naturally ferromagnetic and it can be separated at very low magnetic intensities [34]. Additionally, some hematite was also detected by XRD. Ilmenite appeared from 0.05 T until 0.4 T, as it is a paramagnetic mineral. Some

other works have separated ilmenite from sands using magnetic separation; however, these works have not specified the magnetic field intensity [13,34,35]. Nonetheless, Kim and Jeong [16] separated ilmenite from monazite and quartz by magnetic separation at 0.8 T from a placer deposit. The difference in the magnetic intensities was due to the chemical composition. Indeed, Rosenblum and Brownfield specified a range of the magnetic susceptibilities in which a determined mineral can be separated [27]. In addition, Figure 12 shows monazite was collected from 0.5 T to around 0.9 T. Even monazite was separated at 0.9 T, some of this mineral is considered diamagnetic and it remained in the non-magnetic fraction as shown in Table 4 [36]. Finally, zircon was recovered at 0.9 T. Besides, Figure 12 shows a continuous occurrence of quartz from 0.4 T in almost every magnetic fraction. This implies that since quartz was the main gangue of the fine aggregate waste, and each VHM was not pure, as they have some impurities.

**Table 4.** Chemical composition of the final concentrate separated at different magnetic intensities.

Magnetic Fraction	Fraction (wt%)	SiO <sub>2</sub>	Al <sub>2</sub> O <sub>3</sub>	Fe <sub>2</sub> O <sub>3</sub>	CaO	TiO <sub>2</sub>	MnO	P <sub>2</sub> O <sub>5</sub>	ZrO <sub>2</sub>	REO *
0.05 T	17.86	1.7	0.38	88.54	0.36	3.31	0.00	0.13	0.13	0.00
0.05 T to 0.4 T	40.71	22.85	9.64	29.19	6.22	26.28	1.24	0.60	0.11	1.43
0.4 T to 0.9 T	10.00	35.41	13.10	4.44	7.71	5.37	0.11	6.71	0.63	19.50
Non-magnetic	31.43	58.00	7.02	0.88	2.68	3.37	0.04	1.00	23.92	3.63
Final concentrate	100.00	31.38	7.51	28.42	4.21	12.89	0.53	1.25	7.65	3.67

\* rare earth oxides (REO) includes: CeO<sub>2</sub>, Nd<sub>2</sub>O<sub>3</sub>, La<sub>2</sub>O<sub>3</sub>, Y<sub>2</sub>O<sub>3</sub>, HfO<sub>2</sub>, ThO<sub>2</sub>.

With all the data from XRD and XRF of each magnetic fraction, it was decided to choose 3 magnetic fields: 0.05 T for separating magnetite and hematite, 0.4 T for concentrating ilmenite, 0.9 T for splitting monazite, and the 0.9 T non-magnetic fraction was considered as zircon concentrate. The mineral and chemical composition of each fraction was analyzed by XRD and XRF, respectively. The XRD of each magnetic fraction is shown in Figure 13 and the chemical composition is presented in Table 4. According to Figure 13, each fraction was concentrated effectively since each heavy mineral was separated at the chosen magnetic field intensity. However, the impurities were considerable especially in the case of ilmenite and zircon. In the case of zircon, as it is concentrated in the non-magnetic fraction, the principal impurity was quartz, which is also a diamagnetic mineral.

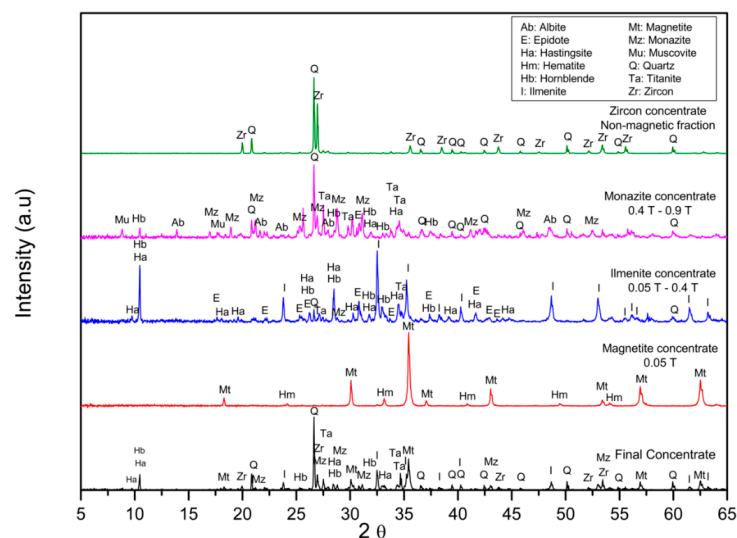


**Figure 13.** X-ray powder diffraction patterns of each concentrate fraction, after being separated using magnetic separation at different magnetic intensities.

In the case of ilmenite, the principal contaminant was hornblende. The gangue has paramagnetic properties and showed attachment at strong magnetic field intensity. As Figure 12 shows, hornblende was recovered from 0.3 T to 0.6 T. In the case of monazite, it was contaminated with quartz and some hornblende, probably because this heavy mineral was attached to the gangue and titanite. That is why the ilmenite concentrate (0.05 T to 0.4 T magnetic fraction), monazite fraction (0.4 T to 0.9 T magnetic fraction), and zircon concentrate (0.9 T non-magnetic fraction) were cleaned by gravity separation and the results are in Figure 14. In the case of magnetite (0.05 T magnetic fraction), since the content was already very high, corroborated with the chemical composition reached in Table 5, and the impurities were undetectable in the XRD shown in Figure 13, hence not further purified.

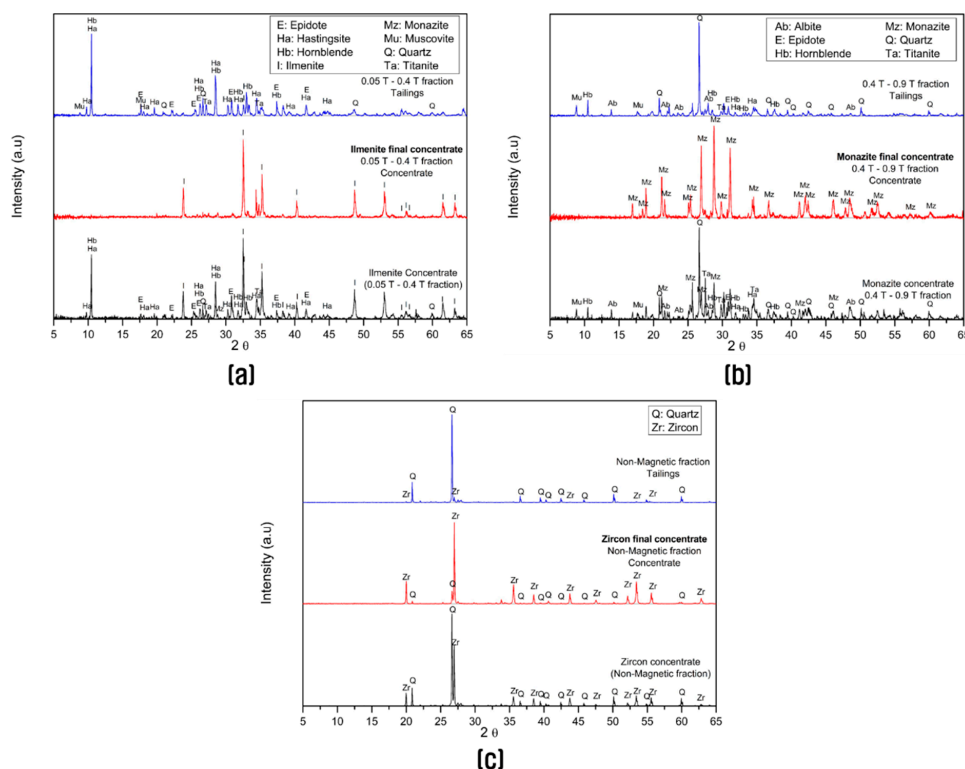


**Figure 14.** XRD patterns of: (a) ilmenite concentrate (0.4 T magnetic fraction), (b) monazite concentrate (0.9 T magnetic fraction), and (c) zircon concentrate (0.9 T non-magnetic fraction); and their respectively concentrate and tailing fractions, after being separated by gravity separation.

**Table 5.** Mineral composition of each final concentrate produced in the current study from dredged fine aggregate waste taken from Pyeongtaek, South Korea.

Concentrate Fraction	Quartz	Hornblende	Ilmenite	Magnetite	REO *	Zircon
Final concentrate	20.04	6.71	26.88	19.27	3.11	9.43
Magnetite	1.7	0.87	2.1	95.1	0	0
Ilmenite	7.59	3.58	84.21	0	2.03	0.36
Monazite	15.96	3.44	8.21	0	45.24	2.21
Zircon	4.3	1.86	1.05	0	1.88	91.76

\* rare earth oxides (REO) includes: CeO<sub>2</sub>, Nd<sub>2</sub>O<sub>3</sub>, La<sub>2</sub>O<sub>3</sub>, Y<sub>2</sub>O<sub>3</sub>, HfO<sub>2</sub>, ThO<sub>2</sub>.

Figure 14a shows the XRD patterns of the ilmenite concentrate after gravity separation. Since the density of ilmenite (4.7 g/cm<sup>3</sup>) is higher than the density of hornblende (3.27 g/cm<sup>3</sup>), the latter goes to the tailings. The gravity separation concentrate has ilmenite while the respective tailings have actinolite (Ca<sub>2</sub>(Mg,Fe)<sub>5</sub>Si<sub>8</sub>O<sub>22</sub>(OH)<sub>2</sub>; JCPDS 41-1366),

hornblende, and quartz. Figure 14b shows the gravity separation for the monazite concentrate. Monazite was separated from quartz and hornblende using gravity separation. The resulting tailings have a high percentage of quartz, and some hornblende, actinolite, and albite. On the other hand, the gravity separation concentrate has monazite and some zircon. Finally, Figure 14c shows the gravity concentration of the 0.9 T non-magnetic fraction. The concentrate has a high percentage of zircon and some traces of quartz. However, the tailings were nearly free from any zircon.

The final concentrations of each extracted heavy mineral are presented in Table 5 and some photographs of the final products are shown in Figure 15. Additionally, Figure 15 shows the fine aggregate waste and final concentrate. All of the collected data were used for developing a process flow diagram of the proposed process, which is pointed out in Figure 16. The magnetite final concentrate had a 23.4% recovery and 95.1 wt% grade. Ilmenite recovery was 55.2%, with a grade of 84.2 wt%, while monazite’s recovery was 59.3% with a rare earth oxide (REO) content of 45.2%. Finally, the zircon grade was 91.8 wt% with a recovery of 70.6%.

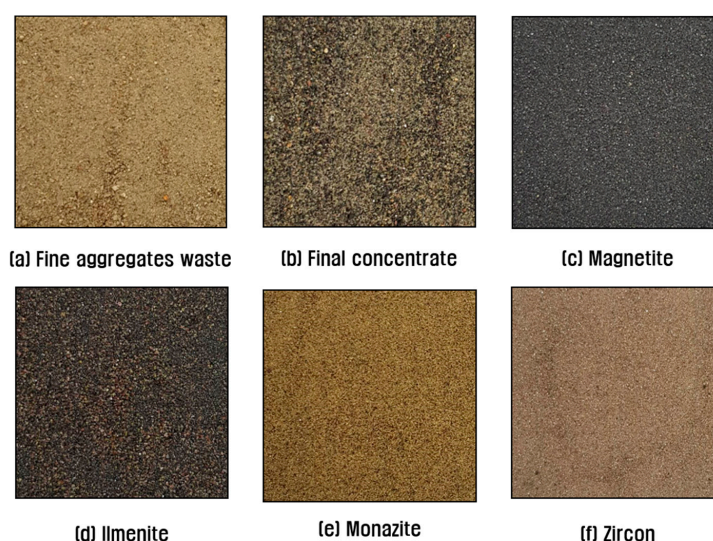


Figure 15. Photographs of: (a) the fine aggregate waste, (b) the final concentrate, and valuable heavy minerals gotten after all the mineral processing (c) magnetite, (d) ilmenite, (e) monazite, and (f) zircon.

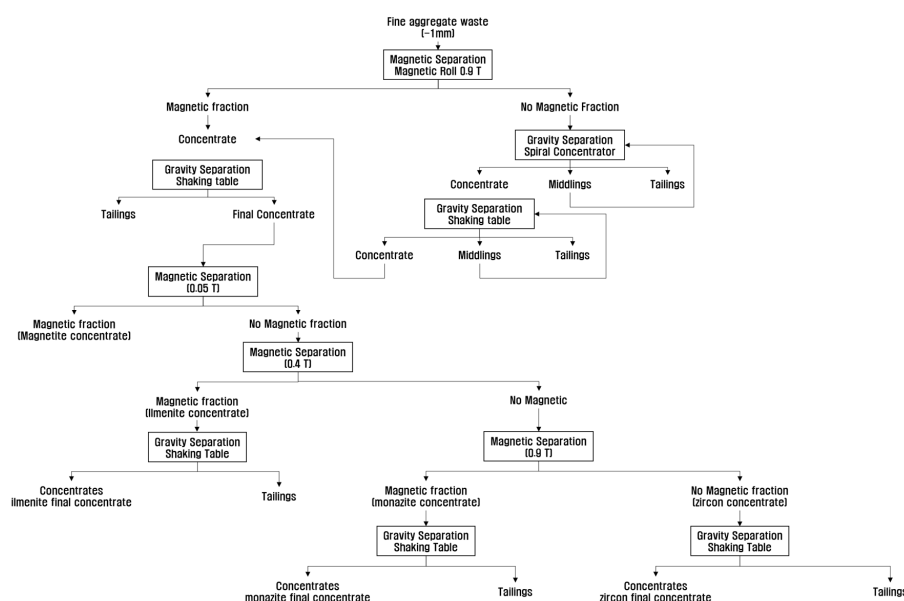


Figure 16. Flow sheet of the proposed process for recovering and purifying VHM contained in the dredged fine aggregate waste from Pyeongtaek, South Korea.

#### 4. Conclusions

In this study, valuable heavy minerals (VHM) contained in the dredged fine aggregate waste from Pyeongtaek South Korea, were effectively separated by a magnetic concentration following gravity separation for the non-magnetic fraction. The raw material had 0.98 wt% of ilmenite, 0.80 wt% of magnetite, 0.18 wt% of zircon, and 618.4 ppm of monazite. The MLA analysis of the heavy fraction confirmed the high liberation degree of each heavy mineral, as they are aggregates. A gravity separation using a Humphrey spiral concentrator can recover 35.76 wt% of ilmenite, 26.55 wt% of magnetite, 48.79 wt% of monazite, and 57.03 wt% of zircon. However, a recirculation of the middlings increased the recovery in ilmenite to 44.05 wt%, magnetite to 36.90 wt%, monazite to 53.76 wt%, and zircon to 69.7 wt%, which means a recirculation of the middlings was required for a better recovery of VHM. Conversely, a magnetic separation of the fine aggregate waste at 0.9 T improved the recovery of the VHM except for the zircon whose concentration decreased. That is the reason why a magnetic separation and a gravity separation of the non-magnetic fraction was developed. The recovery rate of ilmenite was improved to 86.96 wt%, magnetite 85.09 wt%, monazite 91.06 wt%, and zircon 90.82 wt%. The final concentrate was purified by magnetic separation at different magnetic densities. Magnetite was concentrated at 0.05 T with a recovery of 95.1 wt% and a grade of 23.4; ilmenite was at 0.4 T with a recovery of 55.2% and a grade of 84.2 wt%; monazite was separated at 0.9 T with a recovery of 59.3% and a rare earth oxide content of 45.2%. Finally, the non-magnetic fraction concentrated the zircon whose grade was 91.8 wt% and a recovery of 70.6%.

**Author Contributions:** H.-S.K. conceived the idea; H.-S.K. and F.M.-P. designed the experiments; F.M.-P. performed the experiments; H.-S.K. and F.M.-P. analyzed the data; F.M.-P. wrote the original draft; H.-S.K. and F.M.-P. revised, corrected, and edited the manuscript; H.-S.K. got the financial support. All authors have read and agreed to the published version of the manuscript.

**Funding:** This work was supported by the Basic Research Project (GP2015-038-2017(3)), and Basic Research Project (2020-3212-1) of the Korea Institute of Geoscience and Mineral Resources (KIGAM), funded by the Ministry of Science, ICT, and Future Planning of the Republic of Korea.

**Conflicts of Interest:** The authors declare no conflict of interest.

#### References

1. Dehaine, Q.; Filippov, L.O.; Joussmet, R. Rare earths (La, Ce, Nd) and rare metals (Sn, Nb, W) as by-products of kaolin production—Part 2: Gravity processing of micaceous residues. *Miner. Eng.* **2017**, *100*, 200–210. [CrossRef]
2. Schmid, M. Rare Earths in the Trade Dispute between the US and China: A Déjà Vu. Available online: <https://www.intereconomics.eu/contents/year/2019/number/6/article/rare-earths-in-the-trade-dispute-between-the-us-and-china-a-deja-vu.html#footnote-032> (accessed on 17 December 2020).
3. Bohlson, M. The U.S. Rare Earth Saga Continues . . . . Available online: <https://investorintel.com/markets/technology-metals/technology-metals-intel/the-rare-earths-state-of-the-market-july-2019/> (accessed on 17 December 2020).
4. European Commission. *Study on the Review of the List of Critical Raw Materials*; European Commission: Brussels, Belgium, 2017. [CrossRef]
5. Binnemans, K.; Jones, P.T.; Blanpain, B.; Van-Gerven, T.; Yang, Y.; Walton, A.; Buchert, M. Recycling of rare earths: A critical review. *J. Clean. Prod.* **2013**, *51*, 1–22. [CrossRef]
6. Bank of Korea. *2019 Economic Statistics Yearbook*; Bank of Korea: Seoul, Korea, 2019.
7. Route One Communications Ltd. South Korea's Infrastructure Development Is Key to Growth, Aggregates Business International. 2016. Available online: <http://www.aggbusiness.com/sections/market-reports/features/south-koreas-infrastructure-development-is-key-to-growth/> (accessed on 10 January 2018).
8. ASTM International. ASTM C 33-03: Standard specification for Concrete Aggregates. In *Annual Book of ASTM Standards 2010*; ASTM International: Philadelphia, PA, USA, 2010; pp. 1–9.
9. Kosmatka, S.; Wilson, M. Chapter 6 Aggregates for concrete. In *Design and Control of Concrete Mixtures*, 15th ed.; Portland Cement Association: Skokie-Illinois, IL, USA, 2011; pp. 95–102.
10. Rahman, M.A.; Pownceby, M.I.; Haque, N.; Bruckard, W.J.; Zaman, M.N. Valuable heavy minerals from Brahmaputra River sands in Northern Bangladesh. *Appl. Earth Sci.* **2016**, *125*, 174–188. [CrossRef]
11. Abdel-Karim, A.A.; Barakat, M.G. Separation, upgrading, and mineralogy of placer magnetite in the black sands, northern coast of Egypt. *Arab. J. Geosci.* **2017**, *10*. [CrossRef]



12. Philander, C.; Rozendaal, A. A process mineralogy approach model refinement for the Namakwa Sands heavy minerals operations, west coast of South Africa. *Miner. Eng.* **2014**, *65*, 9–16. [[CrossRef](#)]
13. Rejith, R.G.; Sundararajan, M. Combined magnetic, electrostatic, and gravity separation techniques for recovering strategic heavy minerals from beach sands. *Mar. Georesources. Geotechnol.* **2018**, *35*, 959–965. [[CrossRef](#)]
14. Frihy, O.; Deabes, E.; Moufaddal, W.; El-Shahat, A. Recycling of coastal dredged sediments from the Northern Nile Delta, Egypt, for Heavy Minerals Exploitation. *Mar. Georesources Geotechnol.* **2015**, *33*, 408–418. [[CrossRef](#)]
15. Babu, N.; Vasumathi, N.; Rao, R.B. Recovery of Ilmenite and Other Heavy Minerals from Teri Sands (Red Sands) of Tamil Nadu, India. *JMMCE J. Miner. Mater. Charact. Eng.* **2009**, *8*, 149–159. [[CrossRef](#)]
16. Kim, K.; Jeong, S. Separation of Monazite from Placer Deposit by Magnetic Separation. *Minerals* **2019**, *9*, 149. [[CrossRef](#)]
17. Jordens, A.; Sheridan, R.S.; Rowson, N.A.; Waters, K.R. Processing a rare earth mineral deposit using gravity and magnetic separation. *Miner. Eng.* **2014**, *38*, 9–18. [[CrossRef](#)]
18. Jordens, A.; Marion, C.; Langlois, R.; Grammatikopoulos, T.; Sheridan, R.S.; Teng, C.; Demers, H.; Gauvin, R.; Rowson, N.A.; Waters, K.E. Beneficiation of the Nechalacho rare earth deposit. Part 2: Characterisation of products from gravity and magnetic separation. *Miner. Eng.* **2016**, *99*, 96–110. [[CrossRef](#)]
19. Yang, X.; Makkonen, H.T.; Pakkanen, L. Rare Earth Occurrences in Streams of Processing a Phosphate Ore. *Minerals* **2019**, *9*, 262. [[CrossRef](#)]
20. Jordens, A.; Cheng, Y.P.; Waters, K.E. A review of the beneficiation of rare earth element bearing minerals. *Miner. Eng.* **2013**, *41*, 97–114. [[CrossRef](#)]
21. Zhai, J.; Chen, P.; Wang, H.; Hu, Y.; Sun, W. Floatability improvement of Ilmenite Using Attrition-Scrubbing as a Pretreatment method. *Minerals* **2017**, *7*, 13. [[CrossRef](#)]
22. Iranmanesh, M.; Hulliger, J. Magnetic separation: Its application in mining, waste purification, medicine, biochemistry and chemistry. *Chem. Soc. Rev.* **2017**, *46*, 5925–5934. [[CrossRef](#)]
23. Laxmi, T.; Behera, J.R.; Rao, R.B. Beneficiation Studies on Recovery of Ilmenite from Red Sediments of Badlands Topography, Andhra Pradesh. *Adv. Sci. Lett.* **2016**, *22*, 344–348. [[CrossRef](#)]
24. Sullivan, G.V.; Browning, J.S. Recovery of heavy minerals from Alabama sand and gravel operations. In *Bureau of Mines Nonmetallic Minerals Program Technical Progress Report-22: U.S. Department of the Interior*; National Technical Information Service: Springfield, VA, USA, 1970. Available online: <https://ntrl.ntis.gov/NTRL/dashboard/searchResults/titleDetail/PB190997.xhtml> (accessed on 18 December 2020).
25. ILUKA Resources Limited. Mineral Sands Industry Information. 2015, Updated 2019. Available online: <https://www.iluka.com/CMSPages/GetFile.aspx?guid=bd24ecdc-5b71-4681-9340-87c85555cca5> (accessed on 18 December 2020).
26. Wills, B.A.; Napier-Munn, T.J. *Wills' Mineral Processing Technology: An Introduction to the Practical Aspects of Ore Treatment and Mineral Recovery*, 7th ed.; Elsevier Science & Technology Books: London, UK, 2006; ISBN 0750644508.
27. Rosenblum, S.; Brownfield, I.K. *Magnetic Susceptibilities of Minerals*; US Geological Survey Open-File Report 99-529; US Department of the Interior: Washington, DC, USA, 2000. Available online: <http://pubs.usgs.gov/of/1999/ofr-99-0529/> (accessed on 28 November 2020).
28. Arvidson, B.R. Magnetic Separator Assembly for Use in Material Separator Equipment. U.S. Patent 5 101 980, 11 October 1990. Available online: <https://www.google.ch/patents/US5101980> (accessed on 15 August 2020).
29. Lee, Y.; Cho, M.; Yi, K. In situ U-Pb and Lu-Hf isotopic studies of zircon from the Sancheong-Hadong AMCG suite, Yeongnam Massif, Korea: Implications for the petrogenesis of ~1.86 Ga massif-type anorthosite. *J. Asian Earth Sci.* **2017**, *138*, 629–646. [[CrossRef](#)]
30. Grammatikopoulos, W.M.; Gunning, C. Mineralogical characterization using QEMSCAM of the Nechalacho heavy rare earth metal deposit, Northwest Territories, Canada. *Can. Metall. Q.* **2013**, *52*, 265–277. [[CrossRef](#)]
31. Jordens, A.; Marion, C.; Langlois, R.; Grammatikopoulos, T.; Rowson, N.A.; Waters, K.E. Beneficiation of the Nechalacho rare earth deposit. Part 1: Gravity and magnetic separation. *Miner. Eng.* **2016**, *99*, 111–122. [[CrossRef](#)]
32. Kato, Y. Mineralogical study of weathering products of granodiorite at Shinshiro City (III). *J. Soil Sci. Plant Nutr.* **1965**, *11*, 30–40. [[CrossRef](#)]
33. Korea Mineral Resources Information Services (KOMIS). The Prime, Precious Rare Important and Industrial metal Elements, Monthly Report, October 2017. Available online: [https://www.kores.net/common/pdfPreview.do?fid=trendFile&file\\_seq=2690](https://www.kores.net/common/pdfPreview.do?fid=trendFile&file_seq=2690) (accessed on 10 October 2020).
34. Kropáček, V.; Krs, M.; Janák, F. Magnetism of natural pyrrhotite, haematite and ilmenite. *Stud. Geophys. Geod.* **1971**, *15*, 161–172. [[CrossRef](#)]
35. Patruni, B.M.; King, P.; Rao, J. Ilmenite Recovery from Beach sand minerals rejects using Dry Magnetic Separator (RED). *IJESC* **2016**, *6*, 7678–7692. [[CrossRef](#)]
36. Abaka-Wood, G.; Addai-Mensah, J.; Skinner, W. Magnetic separation of monazite from mixed minerals. In *Proceedings of the CHEMECA Conference, Adelaide, Australia, 25–28 September 2016*; Engineers Australia: Melbourne, Australia, 2016; pp. 596–604. ISBN 9781922107831.